

A Robust Force Controller for an SRM Based Electromechanical Brake System

P. Krishnamurthy, W. Lu, F. Khorrami, A. Keyhani

Abstract—In this paper, we propose a robust nonlinear force controller for a switched reluctance motor (SRM) electromechanical brake system which is a promising replacement for hydraulic brakes in the automotive industry. A detailed model of the motor including current dependent inductance coefficients is used. The load exerted on the motor by the caliper may be modeled as a spring; however, the actual load model is taken to be an unknown nonlinear function of position to allow for uncertainties in the model. Hence, the developed controller works for a wide variety of loads including brake systems. The controller is designed using backstepping and incorporates a novel voltage commutation scheme. The controller does not require knowledge of the mechanical parameters of the motor and the functional forms of the relationships among the motor position, the brake force, and the motor load torque. Moreover, the controller provides significant robustness to uncertainty in the inductances. Furthermore, practical current and voltage constraints are addressed. The performance and robustness of the controller are demonstrated through simulation studies.

I. INTRODUCTION

Considerations of safety, comfort, and fuel efficiency have encouraged the development of “by-wire” mechanisms [1] in the automotive industry over the recent years. The ultimate goal [1] of by-wire mechanisms is to enable any driver to be as “skillful” in maneuvering and stabilizing the car as a professional driver. One such system is the electromechanical brake system used to replace hydraulic brakes. This has prompted efforts on modeling and control of electromechanical brake systems [2–4]. Brake systems in an automobile are shown in Figure 1. The driver’s foot pressure measured by a sensor on the brake pedal is communicated to microcontrollers that relay the signal to the electromechanical brake actuators situated at each wheel. The brake actuators then apply the required pressure at the brake pads to smoothly control the car’s speed. This is in contrast to a conventional car in which a hydraulic system would directly respond to pressure on the brake pedal to squeeze the brake pads. A popular actuator used in brake systems and other electric vehicle applications is the switched reluctance motor (SRM) [5,6]. Considerable effort on design [7–9] and modeling [10–15] of SRMs has been reported in the literature. Position and speed control of SRMs has been considered in [16–21]. A torque ripple controller using iterative learning was designed in [22]. A force controller based on numerically inverting the torque-current relation using a look-up table was proposed in [23]. A cross-section of a brake system showing the motor and the caliper is illustrated in Figure 2.

The first and third authors are with the Control/Robotics Research Laboratory (CRRRL), Department of Electrical and Computer Engineering, Polytechnic University, Brooklyn, NY 11201. The second and fourth authors are with the Department of Electrical Engineering, The Ohio State University, Columbus, OH 43210. Emails: pk@crml.poly.edu, wenzhelu@ece.osu.edu, khorrami@smart.poly.edu, keyhani.1@osu.edu
This work is supported in part by the NSF under grant ECS0105320.

In this paper, we develop a new robust nonlinear force controller for an SRM based electromechanical brake system. We utilize a detailed model of the motor including current dependence of the inductance coefficients. The load is taken to be an unknown nonlinear function of position. The modeling and problem statement are contained in Section II. The controller design is given in Section III. The controller is based on robust backstepping [24] and does not require knowledge of the motor mechanical parameters and the functional forms of the relationships among the motor position, the brake force, and the motor load torque. Moreover, the controller provides significant robustness to uncertainty in the inductances. Implementation issues including practical current and voltage constraints are addressed in Section IV. The performance and robustness of the controller are demonstrated through simulation studies in Section V.

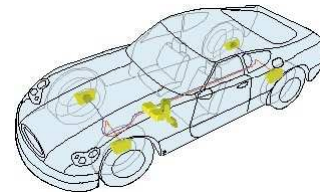


Fig. 1. Brake systems in an automobile [1].

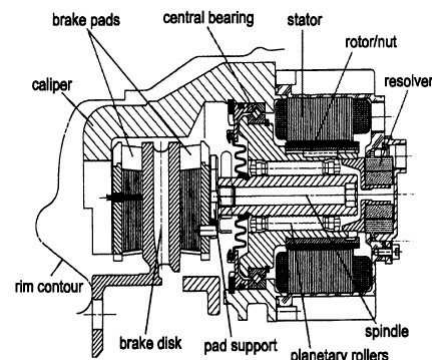


Fig. 2. Cross-section of a brake system [2].

II. MODELING AND PROBLEM STATEMENT

In this section, we develop the model of the SRM brake system. The mechanical dynamics of the motor are given by

$$J\ddot{\theta} = \tau - D\omega - \tau_L \quad (1)$$

where J is the rotational inertia of the motor, D is the viscous friction coefficient, θ is the motor position, ω is the velocity, τ_L is the load torque, and τ is the generated electromechanical torque. The total electromechanical torque τ is given by $\tau = \sum_{j=1}^N \tau_j(\theta, i_j)$ where N is the number of

phases, τ_j is the torque contribution of the j^{th} phase, and i_j is the current in the j^{th} phase. The torque τ_j is given by

$$\tau_j(\theta, i_j) = \int_0^i \frac{\partial L_j(\theta, i_j)}{\partial \theta} i_j di_j \quad (2)$$

where L_j is the inductance associated with the j^{th} phase. The phase inductance L_j is, in general, nonlinear but periodic in θ . Hence, it can be represented as a Fourier series in θ with the coefficients being functions of the current i_j . Retaining, for instance, the first three terms of the Fourier series expansion, we obtain

$$\begin{aligned} L_j(\theta, i_j) = & L_{0,j}(i_j) + L_{1,j}(i_j) \cos\left(N_r(\theta - (j-1)\frac{2\pi}{NN_r})\right) \\ & + L_{2,j}(i_j) \cos\left(2N_r(\theta - (j-1)\frac{2\pi}{NN_r})\right) \end{aligned} \quad (3)$$

where N_r is the number of rotor poles. Defining $L_{a,j}(i_j)$ to be the inductance at aligned position, L_u to be inductance at the unaligned position¹, and $L_{m,j}(i_j)$ to be the inductance at the midway position (between aligned and unaligned),

$$\begin{aligned} L_{a,j}(i_j) &= L_{0,j}(i_j) + L_{1,j}(i_j) + L_{2,j}(i_j) \\ L_u &= L_{0,j}(i_j) - L_{1,j}(i_j) + L_{2,j}(i_j) \\ L_{m,j}(i_j) &= L_{0,j}(i_j) - L_{2,j}(i_j). \end{aligned} \quad (4)$$

Hence,

$$\begin{aligned} L_{0,j}(i_j) &= \frac{1}{2} \left[\frac{1}{2} (L_{a,j}(i_j) + L_u) + L_{m,j}(i_j) \right] \\ L_{1,j}(i_j) &= \frac{1}{2} [L_{a,j}(i_j) - L_u] \\ L_{2,j}(i_j) &= \frac{1}{2} \left[\frac{1}{2} (L_{a,j}(i_j) + L_u) - L_{m,j}(i_j) \right]. \end{aligned} \quad (5)$$

The inductance coefficients $L_{a,j}(i_j)$ and $L_{m,j}(i_j)$ are modeled as polynomial functions of the current i_j :

$$L_{a,j}(i_j) = \sum_{n=0}^k a_n i_j^n, \quad L_{m,j}(i_j) = \sum_{n=0}^k b_n i_j^n \quad (6)$$

with k being a nonnegative integer. The torque expression (2) reduces to

$$\begin{aligned} \tau_j(\theta, i_j) = & -\frac{N_r}{4} i_j^2 \left[(L_{a,j}^{**}(i_j) - L_u) \sin\left(N_r(\theta - (j-1)\frac{2\pi}{NN_r})\right) \right. \\ & + (L_{a,j}^{**}(i_j) + L_u - 2L_{m,j}^{**}(i_j)) \\ & \left. \times \sin\left(2N_r(\theta - (j-1)\frac{2\pi}{NN_r})\right) \right] \end{aligned} \quad (7)$$

$$L_{a,j}^{**}(i_j) = \sum_{n=0}^k \frac{2}{n+2} a_n i_j^n, \quad L_{m,j}^{**}(i_j) = \sum_{n=0}^k \frac{2}{n+2} b_n i_j^n. \quad (8)$$

The electrical dynamics of the SRM are given by

$$v_j = Ri_j + \frac{d}{dt} \lambda_j(\theta, i_j) \quad (9)$$

where v_j and λ_j are the voltage and flux, respectively, associated with the j^{th} phase and R is the phase resistance. Using $\lambda_j(\theta, i_j) = L_j(\theta, i_j) i_j$, we obtain

$$v_j = Ri_j + L_j \frac{di_j}{dt} + i_j \left(\frac{\partial L_j}{\partial \theta} \omega + \frac{\partial L_j}{\partial i_j} \frac{di_j}{dt} \right). \quad (10)$$

Hence,

$$\frac{di_j}{dt} = \frac{1}{\left(L_j + i_j \frac{\partial L_j}{\partial i_j} \right)} \left[v_j - Ri_j - i_j \frac{\partial L_j}{\partial \theta} \omega \right]. \quad (11)$$

From physical considerations, it is meaningful to assume

¹Since the machine is unsaturated at the unaligned position, L_u is a constant (independent of i_j).

that the denominator in (11) is positive within the range of operation of the motor, i.e.,

$$L_j + i_j \frac{\partial L_j}{\partial i_j} > \epsilon > 0. \quad (12)$$

Using the inductance model (3),

$$\begin{aligned} \frac{\partial L_j}{\partial \theta} = & -\frac{N_r}{2} \left[(L_{a,j} - L_u) \sin\left(N_r(\theta - (j-1)\frac{2\pi}{NN_r})\right) \right. \\ & + (L_{a,j} + L_u - 2L_{m,j}) \\ & \left. \times \sin\left(2N_r(\theta - (j-1)\frac{2\pi}{NN_r})\right) \right] \end{aligned} \quad (13)$$

$$\begin{aligned} L_j + i_j \frac{\partial L_j}{\partial i_j} = & \frac{1}{2} \left[\frac{1}{2} (L_{a,j} + L_u) + L_{m,j}^* \right] \\ & + \frac{1}{2} (L_{a,j} - L_u) \cos\left(N_r(\theta - (j-1)\frac{2\pi}{NN_r})\right) \\ & + \frac{1}{2} \left[\frac{1}{2} (L_{a,j} + L_u) - L_{m,j}^* \right] \\ & \times \cos\left(2N_r(\theta - (j-1)\frac{2\pi}{NN_r})\right) \end{aligned} \quad (14)$$

$$L_{a,j}^*(i_j) = \sum_{n=0}^k (n+1) a_n i_j^n; \quad L_{m,j}^*(i_j) = \sum_{n=0}^k (n+1) b_n i_j^n. \quad (15)$$

The load torque τ_L seen by the motor is, in general, a nonlinear function of the actuator force F applied at the brake. The dependence of the load torque on the actuator force and the dependence of the actuator force on the motor mechanical variables are governed by the mechanical coupling between the motor and the load. In general,

$$F = \mu_F(\theta), \quad \tau_L = \mu_L(F) \quad (16)$$

with μ_F and μ_L being nonlinear functions. Physically, it is meaningful to assume that μ_F is monotonic and that the slope of the function μ_F is positive and bounded, i.e.,²

$$\underline{\mu}_F \leq \frac{\partial \mu_F}{\partial \theta} \leq \bar{\mu}_F \quad (17)$$

with $\underline{\mu}_F$ and $\bar{\mu}_F$ being positive constants. Furthermore, typically, τ_L is proportional to F with the proportionality constant being essentially the gear ratio of the coupling between the motor shaft and the load. For generality, however, we only require that

$$|\tau_L| \leq \bar{\mu}_L |F| + \hat{\mu}_L \quad (18)$$

with $\bar{\mu}_L$ and $\hat{\mu}_L$ being nonnegative constants.

The control objective is to make the actuator force F track a given reference trajectory F_{ref} . Practically, it is reasonable to consider F_{ref} and its first derivative to be bounded almost everywhere.

III. CONTROLLER DESIGN

In this section, the force controller for the switched reluctance motor brake system is designed using robust backstepping. The backstepping design proceeds by considering lower-dimensional subsystems and designing *virtual* control inputs (or equivalently, state transformations). The virtual control inputs in the first and second steps are ω and τ , respectively. In the third step, the actual control inputs $v_j, j = 1, \dots, N$, appear and can be designed based on the dynamics of the torque which can be derived using (7) as

$$\dot{\tau} = \sum_{j=1}^N \dot{\tau}_j; \quad \dot{\tau}_j = \frac{\partial \tau_j}{\partial \theta} \omega + \frac{\frac{\partial \tau_j}{\partial i_j} \left[v_j - Ri_j - i_j \frac{\partial L_j}{\partial \theta} \omega \right]}{\left(L_j + i_j \frac{\partial L_j}{\partial i_j} \right)} \quad (19)$$

²Without loss of generality, we have assumed that μ_F is monotonically increasing.

where

$$\begin{aligned} \frac{\partial \tau_j}{\partial \theta} &= -\frac{N_r^2}{4} i_j^2 \left[(L_{a,j}^{**} - L_u) \cos \left(N_r(\theta - (j-1) \frac{2\pi}{NN_r}) \right) \right. \\ &\quad \left. + 2(L_{a,j}^{**} + L_u - 2L_{m,j}^{**}) \cos \left(2N_r(\theta - (j-1) \frac{2\pi}{NN_r}) \right) \right] \quad (20) \\ \frac{\partial \tau_j}{\partial i_j} &= -\frac{N_r}{2} i_j \left[(L_{a,j}^{**} - L_u) \sin \left(N_r(\theta - (j-1) \frac{2\pi}{NN_r}) \right) \right. \\ &\quad \left. + (L_{a,j}^{**} + L_u - 2L_{m,j}^{**}) \sin \left(2N_r(\theta - (j-1) \frac{2\pi}{NN_r}) \right) \right] \\ &\quad - \frac{N_r}{4} i_j^2 \left[\frac{\partial L_{a,j}^{**}}{\partial i_j} \sin \left(N_r(\theta - (j-1) \frac{2\pi}{NN_r}) \right) \right. \\ &\quad \left. + \left(\frac{\partial L_{a,j}^{**}}{\partial i_j} - 2 \frac{\partial L_{m,j}^{**}}{\partial i_j} \right) \sin \left(2N_r(\theta - (j-1) \frac{2\pi}{NN_r}) \right) \right]. \quad (21) \end{aligned}$$

Step 1: For the first step, a Lyapunov function $V_1 = (1/2)z_1^2$ is used where

$$z_1 = F - F_{ref} \quad (22)$$

is the force tracking error. Differentiating V_1 , we obtain

$$\dot{V}_1 = -k_1 \frac{\partial \mu_F}{\partial \theta} z_1^2 + z_1 z_2 \frac{\partial \mu_F}{\partial \theta} - z_1 \dot{F}_{ref} \quad (23)$$

where

$$z_2 = \omega - \omega^*, \quad \omega^* = -k_1 z_1 \quad (24)$$

and $k_1 > 0$ is a design freedom. Here, in the first step of backstepping, the one-dimensional system $\dot{F} = \frac{\partial \mu_F}{\partial \theta} \omega$ is considered and ω is regarded as the virtual control input. Choosing $\omega = -k_1 z_1 = -k_1(F - F_{ref})$ yields practical tracking. However, since ω is not the actual control input, the error between ω and the *desired* ω is formulated as z_2 . In the second step of backstepping, the torque τ will be regarded as the virtual control input and will be *designed* to make z_2 small, i.e., ω converges to the virtual control law ω^* designed for ω , and hence, F converges to F_{ref} . However, since τ is also not the actual control input, the process is repeated once more by introducing an error z_3 which is the difference between τ and the *desired* τ . At the third step, the control inputs v_j , appear and the control law designed at that step can be implemented. Using (17), (23) reduces to

$$\dot{V}_1 \leq -k_1 \underline{\mu}_F z_1^2 + \bar{\mu}_F |z_1| |z_2| + |z_1| |\dot{F}_{ref}|. \quad (25)$$

Step 2: A new Lyapunov function is defined as

$$V_2 = V_1 + \frac{1}{2c_2} z_2^2 \quad (26)$$

where $c_2 > 0$ is a design freedom. Differentiating (26),

$$\begin{aligned} \dot{V}_2 &\leq -k_1 \underline{\mu}_F z_1^2 + \bar{\mu}_F |z_1| |z_2| + |z_1| |\dot{F}_{ref}| \\ &\quad + \frac{1}{c_2} z_2 \left[\frac{1}{J} (\tau - D\omega - \tau_L) + k_1 \frac{\partial \mu_F}{\partial \theta} \omega - k_1 \dot{F}_{ref} \right] \\ &\leq -k_1 \underline{\mu}_F z_1^2 + \bar{\mu}_F |z_1| |z_2| + |z_1| |\dot{F}_{ref}| \\ &\quad - \frac{k_2}{Jc_2} z_2^2 + \frac{1}{Jc_2} |z_2| |z_3| + \frac{D}{Jc_2} |z_2| [|z_2| + k_1 |z_1|] \\ &\quad + \frac{1}{Jc_2} |z_2| [\bar{\mu}_L (|z_1| + |F_{ref}|) + \hat{\mu}_L] \\ &\quad + \frac{k_1}{c_2} \bar{\mu}_F |z_2| [|z_2| + k_1 |z_1|] + \frac{k_1}{c_2} |z_2| |\dot{F}_{ref}| \quad (27) \end{aligned}$$

where

$$z_3 = \tau - \tau^* \quad (28)$$

$$\tau^* = -k_2 z_2 = -k_2 [\omega + k_1 (F - F_{ref})] \quad (29)$$

with $k_2 > 0$ being a controller gain free to be picked by the designer.

Step 3: For the third and final step of backstepping, we use the Lyapunov function

$$V_3 = V_2 + \frac{1}{2c_3} z_3^2 \quad (30)$$

where $c_3 > 0$ is a design freedom. Differentiating (30) and using (27), we have

$$\begin{aligned} \dot{V}_3 &\leq -k_1 \underline{\mu}_F z_1^2 + \bar{\mu}_F |z_1| |z_2| + |z_1| |\dot{F}_{ref}| \\ &\quad - \frac{k_2}{Jc_2} z_2^2 + \frac{1}{Jc_2} |z_2| |z_3| + \frac{D}{Jc_2} |z_2| [|z_2| + k_1 |z_1|] \\ &\quad + \frac{1}{Jc_2} |z_2| [\bar{\mu}_L (|z_1| + |F_{ref}|) + \hat{\mu}_L] \\ &\quad + \frac{k_1}{c_2} \bar{\mu}_F |z_2| [|z_2| + k_1 |z_1|] + \frac{k_1}{c_2} |z_2| |\dot{F}_{ref}| \\ &\quad + \frac{1}{c_3} z_3 \left[\hat{\tau} + k_2 \left(\frac{1}{J} (\tau - D\omega - \tau_L) \right) \right. \\ &\quad \left. + k_1 \frac{\partial \mu_F}{\partial \theta} \omega - k_1 \dot{F}_{ref} \right] \quad (31) \end{aligned}$$

where, for notational convenience, we have introduced $\hat{\tau} = \dot{\tau}$. The control law will first be designed in terms of $\hat{\tau}$. The control laws in terms of the input voltages v_j will then be obtained through a commutation scheme. Designing

$$\hat{\tau} = -k_3 z_3 = -k_3 [\tau + k_2 \omega + k_2 k_1 (F - F_{ref})] \quad (32)$$

with $k_3 > 0$ being a design freedom, (31) reduces to

$$\begin{aligned} \dot{V}_3 &\leq -k_1 \underline{\mu}_F z_1^2 - \frac{k_2}{Jc_2} z_2^2 - \frac{k_3}{c_3} z_3^2 \\ &\quad + |z_1| |z_2| \left[\bar{\mu}_F + \frac{k_1 D}{Jc_2} + \frac{\bar{\mu}_L}{Jc_2} + \frac{k_1^2 \bar{\mu}_F}{c_2} \right] \\ &\quad + |z_1| |z_3| \left[\frac{k_1 k_2 D}{Jc_3} + \frac{k_2 \bar{\mu}_L}{Jc_3} + \frac{k_1^2 k_2 \bar{\mu}_F}{c_3} \right] \\ &\quad + |z_2| |z_3| \left[\frac{1}{Jc_2} + \frac{k_2^2}{Jc_3} + \frac{k_2 D}{Jc_3} + \frac{k_1 k_2 \bar{\mu}_F}{c_3} \right] \\ &\quad + z_2^2 \left[\frac{D}{Jc_2} + \frac{k_1 \bar{\mu}_F}{c_2} \right] + z_3^2 \left[\frac{k_2}{Jc_3} \right] \\ &\quad + |z_1| |\dot{F}_{ref}| + \frac{\bar{\mu}_L}{Jc_2} |z_2| |F_{ref}| \\ &\quad + \frac{\hat{\mu}_L}{Jc_2} |z_2| + \frac{k_1}{c_2} |z_2| |\dot{F}_{ref}| + \frac{k_2 \bar{\mu}_L}{Jc_3} |z_3| |F_{ref}| \\ &\quad + \frac{k_2 \hat{\mu}_L}{Jc_3} |z_3| + \frac{k_1 k_2}{c_3} |z_3| |\dot{F}_{ref}|. \quad (33) \end{aligned}$$

From (33), it is seen that by picking k_1 , k_2 , k_3 , c_2 , and c_3 appropriately, V_3 satisfies

$$\dot{V}_3 \leq -\gamma V_3 + \chi [F_{ref}^2 + \dot{F}_{ref}^2 + \hat{\mu}_L^2] \quad (34)$$

where $\gamma = \min(k_1 \underline{\mu}_F, k_2/J, k_3)$ and χ is a constant independent of the controller gains k_1 , k_2 , and k_3 . The proof of (34) follows by quadratic overbounding which is standard in the backstepping literature [24] and is omitted here for brevity. From (34), it follows that practical tracking is achieved, i.e., the force tracking error $z_1 = F - F_{ref}$ can be regulated to an arbitrarily small compact set by picking k_1 , k_2 , and k_3 large enough.

To obtain control laws in terms of the input voltages v_j , $j = 1, \dots, N$, to achieve the designed form of $\hat{\tau}$ in (32), the following commutation scheme is used:

$$v_j = \left(L_j + i_j \frac{\partial L_j}{\partial i_j} \right) \tilde{v}_j + R i_j + i_j \frac{\partial L_j}{\partial \theta} \omega \quad (35)$$

$$\tilde{v}_j = \frac{\frac{\partial \tau_j}{\partial i_j} \left[\hat{\tau} - \sum_{j=1}^N \frac{\partial \tau_j}{\partial \theta} \omega \right]}{\sum_{j=1}^N \left(\frac{\partial \tau_j}{\partial i_j} \right)^2}. \quad (36)$$

From (36),

$$\sum_{j=1}^N \tilde{v}_j \frac{\partial \tau_j}{\partial i_j} = \hat{\tau} - \sum_{j=1}^N \frac{\partial \tau_j}{\partial \theta} \omega. \quad (37)$$

The commutation scheme (36) exhibits a singularity when all the currents are zero, i.e., when $i_1 = \dots = i_N = 0$. Since the torque vanishes when all the currents are zero, this singularity is not encountered during normal operation of the motor. However, the commutation scheme must be slightly altered during the initial transient when the motor is powered on. This is done by using the standard technique of incorporating a small positive constant ϵ_τ into the denominator to yield the commutation law

$$\tilde{v}_j = \frac{\frac{\partial \tau_j}{\partial i_j} \left[\hat{\tau} - \sum_{j=1}^N \frac{\partial \tau_j}{\partial \theta} \omega \right]}{\sum_{j=1}^N \left(\frac{\partial \tau_j}{\partial i_j} \right)^2 + \epsilon_\tau}. \quad (38)$$

An alternative would be to commutate the desired torque τ^* into the currents i_j using (7). However, this would require the solution of a nonlinear set of equations in i_1, \dots, i_N since the inductance coefficients are modeled as general k^{th} order polynomials. In the special case in which

$$L_j(\theta, i_j) = L_0 - L_1 \cos \left(N_r(\theta - (j-1) \frac{2\pi}{NN_r}) \right), \quad (39)$$

with L_0 and L_1 being constants, the torque reduces to

$$\tau = \frac{N_r L_1}{2} \sum_{j=1}^N i_j^2 \sin \left(N_r(\theta - (j-1) \frac{2\pi}{NN_r}) \right) \quad (40)$$

which allows a closed-form solution[21] for i_j given a desired torque. The approach in this paper has the advantage of being applicable to the general inductance expression (3) without requiring numerical solution of a nonlinear equation.

The overall controller is given by (22), (24), (28), (32), (35), and (38). The controller design freedoms are k_1, k_2, k_3, c_2 , and c_3 . Noting the controller structure, the control law can be slightly generalized to provide additional damping in the electrical dynamics and to provide more design freedom in shaping the force dynamics:

$$\begin{aligned} \hat{\tau} &= -K_p(F - F_{ref}) - K_d(\dot{F} - \dot{F}_{ref}) \\ &\quad - K_i \int_0^t (F(t_1) - F_{ref}(t_1)) dt_1 - K_\tau \tau - K_\omega \omega \\ \tilde{v}_j &= \frac{\frac{\partial \tau_j}{\partial i_j} \left[\hat{\tau} - \sum_{j=1}^N \frac{\partial \tau_j}{\partial \theta} \omega \right]}{\sum_{j=1}^N \left(\frac{\partial \tau_j}{\partial i_j} \right)^2 + \epsilon_\tau} \\ v_j &= \left(L_j + i_j \frac{\partial L_j}{\partial i_j} \right) \tilde{v}_j + i_j \frac{\partial L_j}{\partial \theta} \omega - K_{cur} i_j \end{aligned} \quad (41)$$

with $K_p, K_d, K_i, K_\tau, K_\omega$, and K_{cur} being controller gains free to be picked by the designer. Note that the controller design does not require the knowledge of the mechanical parameters D and J of the motor. Also, the functional form of $F = \mu_F(\theta)$ and $\tau_L = \mu_L(F)$ are not required to be known. Magnitude bounds on D, J, μ_F , and μ_L are sufficient for picking the controller gains. While the controller utilizes nominal knowledge of the electrical parameters of the motor, the design does provide considerable robustness to uncertainty in the electrical parameters also. This is demonstrated through simulations in Section V.

IV. IMPLEMENTATION ISSUES

In the practical implementation of the controller, certain voltage and current constraints must be addressed. Typical voltage constraints include either a limited range or even

a finite number of achievable voltages. For instance, the switching circuits typically used to drive switched reluctance motors provide only $\pm v_{max}$ with v_{max} being a positive voltage. To handle such a voltage constraint, the control law (41) must be saturated and a Pulse Width Modulation (PWM) scheme must be utilized. The choice of the PWM waveform period must take into account the switching frequency of the SRM driving circuit. This also entails a tradeoff among the PWM waveform period, the closed loop bandwidth, and the number of bits of resolution that the PWM scheme achieves.

Practically, the currents are also constrained to lie in a limited range depending on the amplifiers used to drive the motor. To handle this constraint, the voltages are redesigned to include a current regulation regime. When any of the currents i_j exceeds a certain limit i_{max} , the corresponding voltage v_j is switched from (41) to

$$v_j = -v_{max} \text{sign}(i_j) \text{ if } |i_j| > i_{max}. \quad (42)$$

A similar scheme is used around $i_j = 0$ if the current is constrained to remain positive (as is usually the case due to the use of unipolar amplifiers).

V. SIMULATION RESULTS

In this section, the performance of the controller is verified through simulation studies with a switched reluctance motor with the parameters

$$\begin{aligned} J &= 7.5 \times 10^{-5} \text{ kg-m}^2, \quad D = 0 \text{ kg-m}^2/\text{s} \\ R &= 0.015 \Omega, \quad L_u = 0.13 \text{ mH}, \quad N_r = 6, \quad N = 4. \end{aligned} \quad (43)$$

The first five powers of the currents are included in the inductance coefficients, i.e., $k = 5$. The coefficients $a_0, \dots, a_5, b_0, \dots, b_5$ are taken to be

$$\begin{aligned} a_0 &= .959 \times 10^{-3} H & b_0 &= .442 \times 10^{-3} H \\ a_1 &= -.437 \times 10^{-5} H/A & b_1 &= -.137 \times 10^{-5} H/A \\ a_2 &= .647 \times 10^{-6} H/A^2 & b_2 &= .163 \times 10^{-6} H/A^2 \\ a_3 &= -.273 \times 10^{-7} H/A^3 & b_3 &= -.595 \times 10^{-8} H/A^3 \\ a_4 &= .365 \times 10^{-9} H/A^4 & b_4 &= .718 \times 10^{-10} H/A^4 \\ a_5 &= -.159 \times 10^{-11} H/A^5 & b_5 &= -.290 \times 10^{-12} H/A^5. \end{aligned} \quad (44)$$

The parameters of the motor correspond to the experimental setup (Figure 3) of the SRM at The Ohio State University. This comprises the actuator component of the brake system. Using the standstill test, flux as a function of current and position (Figure 4) and the inductance as a function of current and position (Figure 5) were obtained. The inductance coefficients (44) were obtained using the standstill test results and maximum likelihood estimation. The brake is characterized as

$$F = 2.5[(1.19 \times 10^{16} \hat{\theta} - 4.235 \times 10^{13}) \hat{\theta} + 5.904 \times 10^{10}] \hat{\theta} + 1.43 \times 10^6 \hat{\theta} \quad (45)$$

$$\hat{\theta} = \frac{\theta}{28} \left(\frac{0.00125}{\pi} \right) \quad (46)$$

$$\tau_L = \frac{F}{2.5} \frac{1}{28} \left(\frac{0.00125}{\pi} \right). \quad (47)$$

The relation (46) is obtained from the gear and rotary-to-linear mechanism while (45) is the force characteristic of the caliper. The gain of the force transducer is 2.5.

The force reference trajectory is specified to be 2000 N till 0.1 s and 1700 N after that. The voltages are constrained to take on one of two values ± 12 V. The currents are constrained to be maintained in the range $[0, 65]$ A. The value i_{max} at which the control law switches to the current regulation controller (42) is picked to be 60 A. The parameters of the controller were chosen to be $K_p = 20, K_d = 0.002,$



Fig. 3. Experimental setup at The Ohio State University.

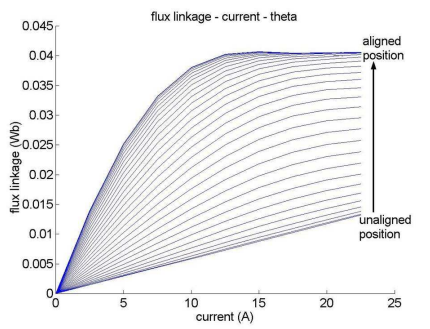


Fig. 4. Flux profile obtained from standstill test results.

$K_i = 2$, $K_\tau = 3500$, $K_\omega = 85$, $K_{cur} = 1$. The simulation results are shown in Figures 6-8. The force, force tracking error, generated electromechanical torque, load torque, position, and velocity are shown in Figure 6. The currents and voltages are shown in Figure 7 and a time segment of the steady state force tracking error is shown in Figure 8. It is seen that the current and voltage constraints are maintained. Both the transient and the steady-state performance are good with the steady-state error being less than 5.5 N.

To demonstrate the robustness of the controller, we consider the case in which only the constant term in the inductance expressions is available for use in the controller. The plant simulation model incorporates five powers of currents as shown in (44). Retaining only the constant term in the inductance expression corresponds to maximum (attained when current = 65 A) errors of 66.3% and 25% in $L_{a,j}(i_j)$ and $L_{m,j}(i_j)$, respectively. Furthermore, the load is changed to include a cascaded first-order linear block with gain 1.1 and time constant 2 ms. The simulation results are shown

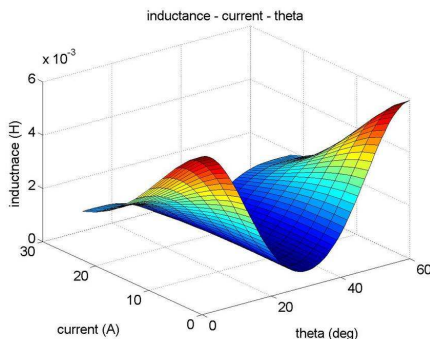


Fig. 5. Inductance profile obtained from standstill test results.

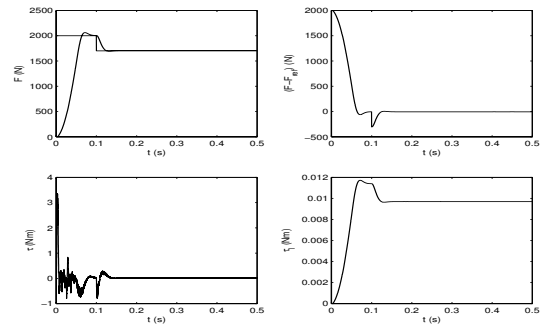


Fig. 6. Simulation results: F , $F - F_{ref}$, τ , τ_L , θ , ω .

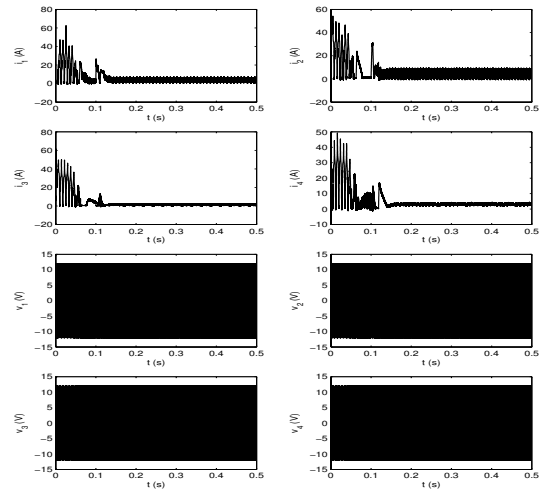


Fig. 7. Simulation results: currents and voltages.

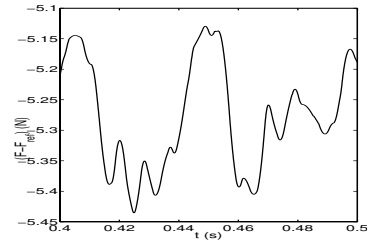


Fig. 8. Simulation results: Steady-state force tracking error.

in Figures 9, 10, and 11. It is seen that the performance is retained (with the steady-state error slightly increased to 6.35 N) in spite of the mismatch of inductances and unmodeled dynamic effects in the load.

VI. CONCLUSION

We proposed a robust nonlinear force controller for an SRM based electromechanical brake system. A detailed model of the motor including current dependence of the inductance coefficients was used. The load was taken to be an unknown nonlinear function of position. The controller was designed via a backstepping procedure and utilized a novel voltage commutation scheme. The controller provides

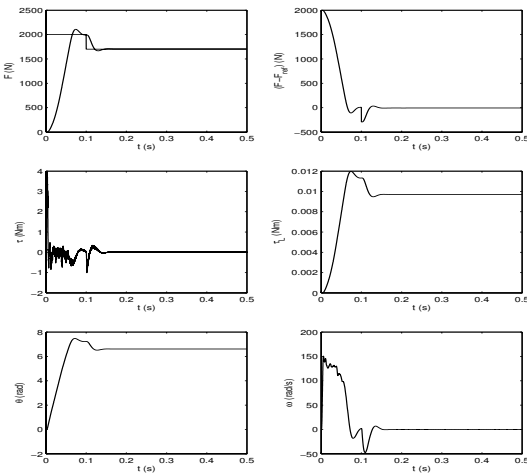


Fig. 9. Simulation results (robustness analysis): F , $F - F_{ref}$, τ , τ_L , θ , ω .

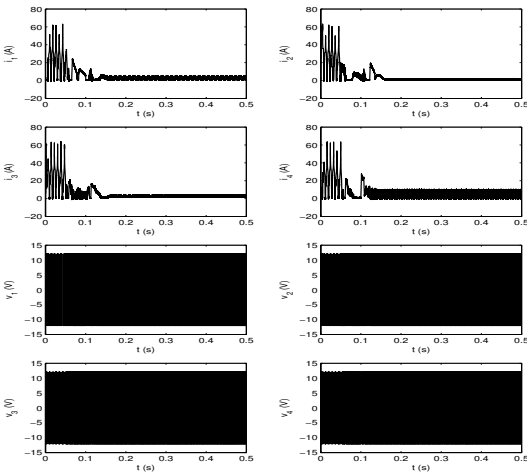


Fig. 10. Simulation results (robustness analysis): currents and voltages.

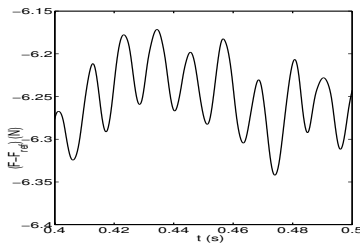


Fig. 11. Simulation results (robustness analysis): Steady-state force tracking error.

four-quadrant operation (i.e., supports forward and backward motoring and braking regimes of operation). The controller does not require knowledge of the mechanical parameters of the motor and the functional forms of the relationships among the motor position, the brake force, and the motor load torque. Moreover, the controller provides significant robustness to uncertainty in the inductances. The proposed controller design can also be extended to brake systems using other types of motors. Implementation issues including current and voltage constraints were also addressed. The performance and robustness of the controller were demonstrated through simulation studies. Experimental implementation of the proposed controller on the testbed at The Ohio State University forms the subject of future work (which would require acquisition of an actual caliper).

REFERENCES

- [1] E. A. Bretz, "By-wire cars turn the corner," *IEEE Spectrum*, vol. 38, pp. 68–73, Apr. 2001.
- [2] R. Schwarz, R. Isermann, J. Bohm, J. Nell, and P. Rieth, "Modeling and control of an electromechanical disk brake," in *Proc. of the Society of Automotive Engineering (SAE) Technical Paper Series 980600, International Congress and Exposition*, (Detroit, MI), Feb. 1998.
- [3] M. Gunzert and A. Nagele, "Component-based development and verification of safety critical software for a brake-by-wire system with synchronous software components," in *Proc. of the International Symposium on Software Engineering for Parallel and Distributed Systems*, (Los Angeles, CA), pp. 134–145, May 1999.
- [4] M. Kees, K. J. Burnham, F. P. Lockett, J. H. Tabor, and R. A. Williams, "Hydraulic actuated brake and electromechanically actuated brake systems," in *Proc. of the IEE International Conf. on Advanced Driver Assistance Systems (ADAS'01)*, pp. 43–47, Sep. 2001.
- [5] R. B. Inderka, M. Menne, and R. W. A. A. D. Doncker, "Control of switched reluctance drives for electric vehicle applications," *IEEE Trans. on Industrial Electronics*, vol. 49, pp. 48–53, Feb. 2002.
- [6] K. M. Rahman and S. E. Schulz, "Design of high-efficiency and high-torque-density switched reluctance motor for vehicle propulsion," *IEEE Trans. on Industry Applications*, vol. 38, pp. 1500–1507, Nov.-Dec. 2002.
- [7] J. Faiz and J. W. Finch, "Aspects of design optimisation for switched reluctance motors," *IEEE Trans. on Energy Conversion*, vol. 8, pp. 704–713, Dec. 1993.
- [8] Y. Tang, "Characterization, numerical analysis, and design of switched reluctance motors," *IEEE Trans. on Industry Applications*, vol. 33, pp. 1544–1552, Nov.-Dec. 1997.
- [9] B. Fahimi, G. Suresh, and M. Ehsani, "Design considerations of switched reluctance motors: vibration and control issues," in *Proc. of the Industry Applications Conf.*, (Phoenix, AZ), pp. 2259–2266, Oct. 1999.
- [10] B. Fahimi, G. Suresh, J. Mahdavi, and M. Ehsani, "A new approach to model switched reluctance motor drive application to dynamic performance prediction, control and design," in *Proc. of the Electronics Specialists Conf.*, pp. 2097–2102, May 1998.
- [11] S. Mir, I. Husain, and M. E. Elbuluk, "Switched reluctance motor modeling with on-line parameter identification," *IEEE Trans. on Industry Applications*, vol. 34, pp. 776–783, July-Aug. 1998.
- [12] N. J. Nagel and R. D. Lorenz, "Modeling of a saturated switched reluctance motor using an operating point analysis and the unsaturated torque equation," *IEEE Trans. on Industry Applications*, vol. 36, pp. 714–722, May-June 2000.
- [13] B. C. Mecrow, C. Weiner, and A. C. Clothier, "The modeling of switched reluctance machines with magnetically coupled windings," *IEEE Trans. on Industry Applications*, vol. 37, pp. 1675–1683, Nov.-Dec. 2001.
- [14] I. Moson, K. Iwan, and J. Nieznanski, "Circuit-oriented model of the switched reluctance motor for drive systems simulation," in *Proc. of the IEEE Annual Conf. of the Industrial Electronics Society*, pp. 497–501, Nov. 2002.
- [15] W. Lu, A. Keyhani, and A. Fardoun, "Neural network-based modeling and parameter identification of switched reluctance motors," *IEEE Trans. on Energy Conversion*, vol. 18, pp. 284–290, June 2003.
- [16] M. Ilić-Spong, R. Marino, S. Peresada, and D. G. Taylor, "Feedback linearizing control of switched reluctance motors," *IEEE Trans. on Automatic Control*, vol. 32, pp. 371–379, May 1987.
- [17] D. Taylor, "An experimental study on composite control of switched reluctance motors," *IEEE Control Systems Mag.*, pp. 31–36, Feb. 1991.
- [18] J. Carroll and D. Dawson, "Adaptive tracking control of a switched reluctance motor turning an inertial load," in *Proc. of the American Control Conf.*, (San Francisco, CA), pp. 670–674, June 1993.
- [19] R. R. Kohan and S. A. Bortoff, "Adaptive control of variable reluctance motors using spline functions," in *Proc. of the IEEE Conf. on Decision and Control*, (Lake Buena Vista, FL), pp. 1694–1699, Dec. 1994.
- [20] H. Melkote, F. Khorrami, S. Jain, and M. Mattice, "Robust adaptive control of variable reluctance stepper motors," *IEEE Trans. on Control Systems Technology*, vol. 7, pp. 212–221, March 1999.
- [21] F. Khorrami, P. Krishnamurthy, and H. Melkote, *Modeling and Adaptive Nonlinear Control of Electric Motors*. New York: Springer Verlag, 2003.
- [22] N. C. Sahoo, J. X. Xu, and S. K. Panda, "Low torque ripple control of switched reluctance motors using iterative learning," *IEEE Trans. on Energy Conversion*, vol. 16, pp. 318–326, Dec. 2001.
- [23] A. A. Goldenberg, I. Laniado, P. Kuzan, and C. Zhou, "Control of switched reluctance motor torque for force control applications," *IEEE Trans. on Industrial Electronics*, vol. 41, pp. 461–466, Aug. 1994.
- [24] M. Krstić, I. Kanellakopoulos, and P. V. Kokotović, *Nonlinear and Adaptive Control Design*. New York: Wiley, 1995.